Comput Mech (2008) 42:761–773
DOI 10.1007/s00466-008-0274-2

ORIGINAL PAPER

A fast multipole boundary element method for 2D multi-domain elastostatic problems based on a dual BIE formulation

Y. J. Liu

Received: 20 December 2007 / Accepted: 8 March 2008 / Published online: 26 March 2008

Abstract A new fast multipole formulation for the hypersingular BIE (HBIE) for 2D elasticity is presented in this paper based on a complex-variable representation of the kernels, similar to the formulation developed earlier for the conventional BIE (CBIE). A dual BIE formulation using a linear combination of the developed CBIE and HBIE is applied to analyze multi-domain problems with thin inclusions or open cracks. Two pre-conditioners for the fast multipole boundary element method (BEM) are devised and their effectiveness and efficiencies in solving large-scale problems are discussed. Several numerical examples are presented to study the accuracy and efficiency of the developed fast multipole BEM using the dual BIE formulation. The numerical results clearly demonstrate the potentials of the fast multipole BEM for solving large-scale 2D multi-domain elasticity problems. The method can be applied to study composite materials, functionally-graded materials, and micro-electro-mechanical-systems with coupled fields, all of which often involve thin shapes or thin inclusions.

Keywords Boundary element method · Fast multipole method · 2D elasticity · Multiple domains

1 Introduction

In the mid of 1980s, Rokhlin and Greengard [1–3] pioneered the innovative fast multipole method (FMM) that can be used to accelerate the solutions of boundary integral equation/boundary element method (BIE/BEM) by several folds, reducing both the CPU time and memory requirement in FMM accelerated BEM to $O(N)$. Some of the early research on fast multipole BEM in applied mechanics can be found in [4–8], which demonstrate great promises of the fast multipole BEM for solving large-scale engineering problems. A comprehensive review of the fast multipole accelerated BIE/BEM in applied mechanics and the research work up to 2002 can be found in [9].

For 2D elasticity problems, there are several fast multipole BEM approaches developed so far. Greengard et al. [10,11] developed a fast multipole formulation for directly solving the biharmonic equations in 2D elasticity. They applied Sherman's complex variable formulation to solve the biharmonic equation and presented several interesting large-scale problems. Peirce and Napier [4] developed a spectral multipole approach, that shares some common features with the fast multipole methods. In their approach, a set of background grids are generated and Taylor series expansions of the kernels are used to compute the integrals at the grid points. Interpolations of these values give the values at the collocation points. This approach is of order $O(N \log N)$ in computational complexity. Richardson et al. [12] proposed a similar spectral method using both 2D conventional and traction BIEs in the regularized form. Fukui [13,14] studied both the conventional BIE (CBIE) for 2D stress analysis and hypersingular BIE (HBIE) for large-scale crack problems. In his work, he first applied the complex variable representation of the kernels and then employed the multipole expansions in complex variables as originally used for 2D potential problems [3,15]. Liu [16] further studied Fukui's approach and proposed a new set of moments for 2D elasticity CBIE, which yields a very compact and efficient formulation with all the translations being symmetrical regarding the two sets of moments. Large-scale 2D elasticity problems with the total numbers of equations above one million were solved on a laptop computer with 1 GB memory using this new formulation

Y. J. Liu (✉)
Department of Mechanical Engineering, University of Cincinnati, P.O. Box 210072, Cincinnati, OH 45221-0072, USA
e-mail: Yijun.liu@uc.edu

[16]. Wang and Yao [17] also studied crack problems using a dual BIE approach with the CBIE collocating on one surface of a crack and HBIE on the other. They expanded the kernel functions in their original forms using complex Taylor series in an auxiliary way following the approach in [18]. In [19], the authors further studied 2D multi-domain elasticity problems using the CBIE alone for modeling composite materials. In another related work using complex variables [20], Wang et al. presented a fast and accurate algorithm for solving elastostatic problems involving numerous straight cracks and circular inhomogeneities in an infinite plane. To the author's best knowledge, the fast multipole BEM based on a dual BIE formulation has not been applied to solve 2D multi-domain elasticity problems with regular as well as thin inclusions.

In the study of the fast multipole BEM for 2D problems, it has been recognized that the approaches based on expansions of the kernels in complex variables [3,10,15,16] are much more efficient than approaches based on expansions of kernels in real variables. This is because each term in a series of complex variables is an analytic function, and its real and imaginary parts are harmonic functions, which are solutions of linear elastostatic problems. Thus, faster convergence can be achieved with fewer expansion terms in the fast multipole BEM using the complex BIE formulations [3, 10,15,16]. The complex variable approach is extended in this paper to develop a fast multipole BEM for 2D multi-domain elasticity problems based on a dual BIE formulation where a linear combination of the CBIE and HBIE is employed.

In this paper, a new fast multipole BEM approach is presented for 2D multi-domain elasticity problems using a dual BIE formulation based on the work in [16] for 2D single-domain elasticity with the CBIE. First, the dual BIE formulation is presented that involves the CBIE for the displacement and HBIE for the traction. Then, the fast multipole formulations for the CBIE and HBIE are presented, where multipole formulations for the HBIE are derived by taking derivatives of the local expansions of the CBIE using complex variables. All the moments and related M2M, M2L and L2L translations for the HBIE turn out to be identical to those for the CBIE and thus very compact and efficient fast multipole BEM code can be developed using this dual BIE formulation. Two pre-conditioners for the linear system of equations for multi-domain problems are presented and their efficiencies are discussed. Numerical examples are presented and the results clearly demonstrate the effectiveness, accuracy and efficiency of the fast multipole BEM based on the dual BIE formulation for analyzing large-scale 2D multi-domain elasticity problems. Finally, discussions are given on possible improvements of the developed fast multipole BEM for multi-domain problems using the dual BIE formulation and its extensions to other applications.

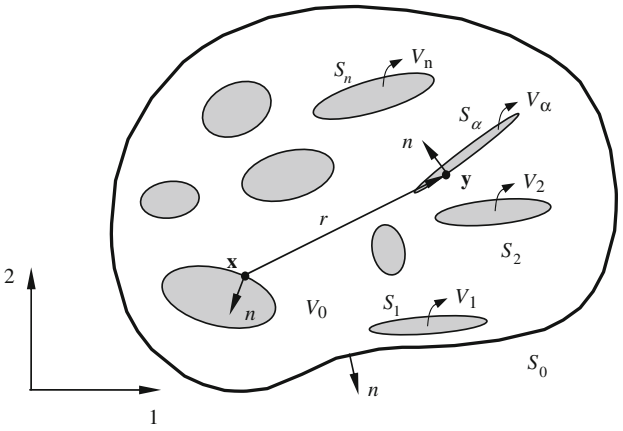

Fig. 1 Matrix domain V_0 and n inclusions

2 Dual BIE formulation for 2D elastostatics

Consider a 2D elastic domain V_0 embedded with n elastic inclusions V_α (Fig. 1). The conventional BIE (CBIE) for matrix domain V_0 is given by [21–25]:

$$\frac{1}{2}u_i(\mathbf{x}) = \int_S \left[U_{ij}(\mathbf{x},\mathbf{y})t_j(\mathbf{y}) - T_{ij}(\mathbf{x},\mathbf{y})u_j(\mathbf{y})\right] dS(\mathbf{y}), \quad \forall \mathbf{x} \in S, \tag{1}$$

where u_i and t_i are the displacement and traction, respectively; $S = \bigcup_{\alpha=0}^{n} S_\alpha$ is the boundary of domain V_0 (Fig. 1) (assuming that S is smooth around $\mathbf{x}$); and the two kernel functions $U_{ij}(\mathbf{x},\mathbf{y})$ and $T_{ij}(\mathbf{x},\mathbf{y})$ in Eq. (1) are the fundamental solution (Kelvin's solution) given by [21–25]:

$$U_{ij}(\mathbf{x},\mathbf{y}) = \frac{1}{8\pi\mu(1-\nu)}\left[(3-4\nu)\delta_{ij}\log\left(\frac{1}{r}\right) + r_{,i}\,r_{,j} - \frac{1}{2}\delta_{ij}\right], \tag{2}$$

$$T_{ij}(\mathbf{x},\mathbf{y}) = -\frac{1}{4\pi(1-\nu)r}\left\{\frac{\partial r}{\partial n}\left[(1-2\nu)\delta_{ij} + 2r_{,i}\,r_{,j}\right] - (1-2\nu)\left(r_{,i}\,n_j - r_{,j}\,n_i\right)\right\}, \tag{3}$$

for the plane strain case, in which μ is the shear modulus, ν Poisson's ratio, $r = r(\mathbf{x},\mathbf{y})$ the distance between the source point $\mathbf{x}$ and field point $\mathbf{y}$, n_i component of the outward normal at $\mathbf{y}$ (Fig. 1), and $(\ )_{,i} = \partial(\ )/\partial y_i$. The constant term $-1/2\delta_{ij}$ in expression (2), which does not affect the BIE solution, is added for the convenience in the complex variable BIE formulation [16]. In BIE (1), the integral with U kernel is a weakly-singular integral, while the one with the T kernel is a Cauchy principal-value (CPV) integral.

For each inclusion, the conventional BIE can be written as:

$$\frac{1}{2}u_i^{(\alpha)}(\mathbf{x}) = \int_{S_\alpha} \left[U_{ij}^{(\alpha)}(\mathbf{x},\mathbf{y})t_j^{(\alpha)}(\mathbf{y}) - T_{ij}^{(\alpha)}(\mathbf{x},\mathbf{y})u_j^{(\alpha)}(\mathbf{y})\right] dS(\mathbf{y}), \quad \forall \mathbf{x} \in S_\alpha, \tag{4}$$

for $\alpha = 1, 2, \ldots, n$, in which $u_i^{(\alpha)}$ and $t_i^{(\alpha)}$ are the displacement and traction, respectively, for inclusion α; and $U_{ij}^{(\alpha)}(\mathbf{x},\mathbf{y})$ and $T_{ij}^{(\alpha)}(\mathbf{x},\mathbf{y})$ are given by Eqs. (2) and (3), respectively, with the shear modulus, Poisson's ratio and outward normal for inclusion α.

Taking derivatives of BIE (1) (with $\mathbf{x}$ inside V_0), applying the stress–strain relation, and letting the source point $\mathbf{x}$ approach the boundary of V_0 [26,27], one can obtain the traction (hypersingular) BIE (HBIE) for the matrix domain V_0 as follows:

$$\frac{1}{2}t_i(\mathbf{x}) = \int_S \left[K_{ij}(\mathbf{x},\mathbf{y})t_j(\mathbf{y}) - H_{ij}(\mathbf{x},\mathbf{y})u_j(\mathbf{y})\right] dS(\mathbf{y}), \quad \forall \mathbf{x} \in S, \tag{5}$$

where the two kernels are:

$$K_{ij}(\mathbf{x},\mathbf{y}) = \frac{1}{4\pi(1-\nu)r}\left[(1-2\nu)(\delta_{ij}r_{,k} + \delta_{jk}r_{,i} - \delta_{ik}r_{,j}) + 2r_{,i}\,r_{,j}\,r_{,k}\right] n_k(\mathbf{x}), \tag{6}$$

$$H_{ij}(\mathbf{x},\mathbf{y}) = \frac{\mu}{2\pi(1-\nu)r^2}\left\{2\frac{\partial r}{\partial n}\left[(1-2\nu)\delta_{ik}r_{,j} + \nu(\delta_{ij}r_{,k} + \delta_{jk}r_{,i}) - 4r_{,i}\,r_{,j}\,r_{,k}\right] + 2\nu(n_i r_{,j}\,r_{,k} + n_k r_{,i}\,r_{,j}) - (1-4\nu)\delta_{ik}n_j + (1-2\nu)\left(2n_j r_{,i}\,r_{,k} + \delta_{ij}n_k + \delta_{jk}n_i\right)\right\} n_k(\mathbf{x}), \tag{7}$$

with $n_i(\mathbf{x})$ being the normal at source point $\mathbf{x}$ (Fig. 1). In BIE (5), the integral with kernel K is a CPV integral, while the one with kernel H is a Hadamard finite-part (HFP) integral [27,28].

For each inclusion, the hypersingular BIE can be written as:

$$\frac{1}{2}t_i^{(\alpha)}(\mathbf{x}) = \int_{S_\alpha} \left[K_{ij}^{(\alpha)}(\mathbf{x},\mathbf{y})t_j^{(\alpha)}(\mathbf{y}) - H_{ij}^{(\alpha)}(\mathbf{x},\mathbf{y})u_j^{(\alpha)}(\mathbf{y})\right] dS(\mathbf{y}), \forall \mathbf{x} \in S_\alpha, \tag{8}$$

for $\alpha = 1, 2, \ldots, n$, in which $K_{ij}^{(\alpha)}(\mathbf{x},\mathbf{y})$ and $H_{ij}^{(\alpha)}(\mathbf{x},\mathbf{y})$ are given by Eqs. (6) and (7), respectively, using the shear modulus, Poisson's ratio and outward normal for inclusion α.

A dual BIE (CHBIE) formulation using a linear combination of the CBIE and HBIE can be written as:

$$\text{CBIE} + \beta\,\text{HBIE} = 0, \tag{9}$$

for the matrix domain using CBIE (1) and HBIE (5), and for each inclusion α using CBIE (4) and HBIE (8), where β is the coupling constant. In this study, the choice of β equal to the size of a typical element in the mesh (and divided by the Young's modulus) has been found to be quite effective for all the cases. More discussions on the selection of β can be found in [29–34] for other cases. Dual BIE formulations have been found to be very effective and efficient for solving acoustic wave, elastic wave, potential and electrostatic problems [29–34]. Dual BIE formulations are especially beneficial to the fast multipole BEM since they provide better conditioning for the BEM systems of equations than the CBIE formulation and thus can facilitate faster convergence (see, e.g., [33–35]).

The discretized form of the multi-domain CHBIE (9), using CBIE (1) and HBIE (5) for the matrix domain and CBIE (4) and HBIE (8) for the inclusions, can be written as follows:

$$\begin{array}{cc} & \begin{matrix} S_0 & S_1 & S_2 & \cdots & S_n \end{matrix} \\ \begin{matrix} \text{Matrix} \\ \\ \\ \\ \\ \text{Inclusions} \\ \\ \\ \\ \end{matrix} & \begin{bmatrix} \mathbf{A}_{00} & \mathbf{A}_{01} & \mathbf{A}_{02} & \cdots & \mathbf{A}_{0n} & -\mathbf{B}_{01} & -\mathbf{B}_{02} & \cdots & -\mathbf{B}_{0n} \\ \mathbf{A}_{10} & \mathbf{A}_{11} & \mathbf{A}_{12} & \cdots & \mathbf{A}_{1n} & -\mathbf{B}_{11} & -\mathbf{B}_{12} & \cdots & -\mathbf{B}_{1n} \\ \mathbf{A}_{20} & \mathbf{A}_{21} & \mathbf{A}_{22} & \cdots & \mathbf{A}_{2n} & -\mathbf{B}_{21} & -\mathbf{B}_{22} & \cdots & -\mathbf{B}_{2n} \\ \vdots & \vdots & \vdots & \ddots & \vdots & \vdots & \vdots & \ddots & \vdots \\ \mathbf{A}_{n0} & \mathbf{A}_{n1} & \mathbf{A}_{n2} & \cdots & \mathbf{A}_{nn} & -\mathbf{B}_{n1} & -\mathbf{B}_{n2} & \cdots & -\mathbf{B}_{nn} \\ \mathbf{0} & \mathbf{A}_1^f & \mathbf{0} & \cdots & \mathbf{0} & \mathbf{B}_1^f & \mathbf{0} & \cdots & \mathbf{0} \\ \mathbf{0} & \mathbf{0} & \mathbf{A}_2^f & \cdots & \mathbf{0} & \mathbf{0} & \mathbf{B}_2^f & \cdots & \mathbf{0} \\ \vdots & \vdots & \vdots & \ddots & \vdots & \vdots & \vdots & \ddots & \vdots \\ \mathbf{0} & \mathbf{0} & \mathbf{0} & \cdots & \mathbf{A}_n^f & \mathbf{0} & \mathbf{0} & \cdots & \mathbf{B}_n^f \end{bmatrix} \end{array}$$

$$\begin{Bmatrix} \mathbf{u}_0 \\ \mathbf{u}_1 \\ \mathbf{u}_2 \\ \vdots \\ \mathbf{u}_n \\ \mathbf{t}_1 \\ \mathbf{t}_2 \\ \vdots \\ \mathbf{t}_n \end{Bmatrix} = \begin{bmatrix} \mathbf{B}_{00} \\ \mathbf{B}_{10} \\ \mathbf{B}_{20} \\ \vdots \\ \mathbf{B}_{n0} \\ \mathbf{0} \\ \mathbf{0} \\ \vdots \\ \mathbf{0} \end{bmatrix} \{\mathbf{t}_0\}, \tag{10}$$

in which $\mathbf{u}_0$ and $\mathbf{t}_0$ are the displacement and traction vector on the outer boundary S_0, $\mathbf{u}_i$ and $\mathbf{t}_i$ the displacement and traction vector on the interface S_i from the matrix domain, and $\mathbf{A}_{ij}$ and $\mathbf{B}_{ij}$ the coefficient submatrices from the matrix domain, while $\mathbf{A}_i^f$ and $\mathbf{B}_i^f$ the coefficient submatrices from inclusion i. On the interface, displacement continuity and traction equilibrium conditions have been assumed.

Rearranging the terms in Eq. (10), an alternative form of the BEM system of equations is:

$$
\begin{array}{l}
\text{Matrix } S_0 \\
\text{Matrix } S_1 \\
\text{Inclusion } S_1 \\
\text{Matrix } S_2 \\
\text{Inclusion } S_2 \\
\vdots \\
\text{Matrix } S_n \\
\text{Inclusion } S_n
\end{array}
\begin{bmatrix}
\mathbf{A}_{00} & \mathbf{A}_{01} & -\mathbf{B}_{01} & \mathbf{A}_{02} & -\mathbf{B}_{02} & \cdots & \mathbf{A}_{0n} & -\mathbf{B}_{0n} \\
\mathbf{A}_{10} & \mathbf{A}_{11} & -\mathbf{B}_{11} & \mathbf{A}_{12} & -\mathbf{B}_{12} & \cdots & \mathbf{A}_{1n} & -\mathbf{B}_{1n} \\
\mathbf{0} & \mathbf{A}_1^f & \mathbf{B}_1^f & \mathbf{0} & \mathbf{0} & \cdots & \mathbf{0} & \mathbf{0} \\
\mathbf{A}_{20} & \mathbf{A}_{21} & -\mathbf{B}_{21} & \mathbf{A}_{22} & -\mathbf{B}_{22} & \cdots & \mathbf{A}_{2n} & -\mathbf{B}_{2n} \\
\mathbf{0} & \mathbf{0} & \mathbf{0} & \mathbf{A}_2^f & \mathbf{B}_2^f & \cdots & \mathbf{0} & \mathbf{0} \\
\vdots & \vdots & \vdots & \vdots & \vdots & \ddots & \vdots & \vdots \\
\mathbf{A}_{n0} & \mathbf{A}_{n1} & -\mathbf{B}_{n1} & \mathbf{A}_{n2} & -\mathbf{B}_{n2} & \cdots & \mathbf{A}_{nn} & -\mathbf{B}_{nn} \\
\mathbf{0} & \mathbf{0} & \mathbf{0} & \mathbf{0} & \mathbf{0} & \cdots & \mathbf{A}_n^f & \mathbf{B}_n^f
\end{bmatrix}
$$

$$
\times \begin{Bmatrix} \mathbf{u}_0 \\ \mathbf{u}_1 \\ \mathbf{t}_1 \\ \mathbf{u}_2 \\ \mathbf{t}_2 \\ \vdots \\ \mathbf{u}_n \\ \mathbf{t}_n \end{Bmatrix} = \begin{bmatrix} \mathbf{B}_{00} \\ \mathbf{B}_{10} \\ \mathbf{0} \\ \mathbf{B}_{20} \\ \mathbf{0} \\ \vdots \\ \mathbf{B}_{n0} \\ \mathbf{0} \end{bmatrix} \{\mathbf{t}_0\}. \tag{11}
$$

Both systems of Eqs. in (10) and (11) will be tested with the fast multipole BEM to investigate the computational efficiencies. In solving the above linear systems, the matrix–vector multiplications when using the GMRES iterative solver will be evaluated using the fast multipole method which will be discussed next.

3 Fast multipole BEM for the dual BIE formulation

The fast multipole algorithms for solving general 2D elasticity problems using CBIE (1) have been described in details in [16]. These results are summarized in the following for completeness. Then the treatment of HBIE (5) is presented in this section.

In [16], it is shown that the two integrals in the CBIE for 2D elasticity can be represented in complex variables readily if the fundamental solution $U_{ij}(\mathbf{x}, \mathbf{y})$ and $T_{ij}(\mathbf{x}, \mathbf{y})$ are written in complex forms using the classical results in 2D elasticity for fields due to a point force [36–38]. For example, CBIE (1) can be written in a complex form as follows [16]:

$$
\frac{1}{2}u(z_0) = D_t(z_0) - D_u(z_0), \tag{12}
$$

in which:

$$
\begin{aligned}
D_t(z_0) \equiv & \left[\int_S U_{1j}(\mathbf{x}, \mathbf{y}) t_j(\mathbf{y}) dS(\mathbf{y})\right] \\
& + i\left[\int_S U_{2j}(\mathbf{x}, \mathbf{y}) t_j(\mathbf{y}) dS(\mathbf{y})\right] \\
= & \frac{1}{4\pi\mu(1+\kappa)} \int_S \Big[\kappa G(z_0, z) t(z) - (z_0 - z) \\
& \times \overline{G'(z_0, z) t(z)} + \kappa \overline{G(z_0, z)} t(z)\Big] dS(z),
\end{aligned} \tag{13}
$$

representing the first integral with the U kernel in CBIE (1), and

$$
\begin{aligned}
D_u(z_0) \equiv & \left[\int_S T_{1j}(\mathbf{x}, \mathbf{y}) u_j(\mathbf{y}) dS(\mathbf{y})\right] \\
& + i\left[\int_S T_{2j}(\mathbf{x}, \mathbf{y}) u_j(\mathbf{y}) dS(\mathbf{y})\right] \\
= & -\frac{1}{2\pi(1+\kappa)} \int_S \Big\{\kappa G'(z_0, z) n(z) u(z) - (z_0 - z) \\
& \times \overline{G''(z_0, z) n(z) u(z)} + \overline{G'(z_0, z)} \\
& \times \Big[n(z)\overline{u(z)} + \overline{n(z)} u(z)\Big]\Big\} dS(z),
\end{aligned} \tag{14}
$$

representing the second integral with the T kernel in CBIE (1). In the above equations, $i = \sqrt{-1}$; $\overline{(\ )}$ indicates the complex conjugate; $u = u_1 + iu_2$, $t = t_1 + it_2$ and $n = n_1 + in_2$ are the complex displacement, traction and normal, respectively; $z_0 (= x_1 + ix_2)$ and $z\ (= y_1 + iy_2)$ represent $\mathbf{x}$ and $\mathbf{y}$, respectively; $G(z_0, z) = -\log(z_0 - z)$ the Green's function (in complex form) for 2D potential problems [3,15], $(\ )' \equiv \partial(\ )/\partial z_0$, and $\kappa = 3 - 4\nu$ for the plane strain case.

To derive the complex form of the HBIE (5), one first notes that the real variable traction t_i on the boundary S is given by:

$$
t_i = \sigma_{ij} n_j = \left[\lambda \delta_{ij} u_{k,k} + \mu(u_{i,j} + u_{j,i})\right] n_j, \tag{15}
$$

in which σ_{ij} is the stress tensor and $\lambda = 2\mu\nu/(1 - 2\nu)$ for plane strain problems. It is interesting to note that this relation has a *complex form* as follows:

$$
t(z) = 2\mu\left[\frac{1}{\kappa - 1}\left(\frac{\partial u}{\partial z} + \frac{\partial \overline{u}}{\partial \overline{z}}\right) n + \frac{\partial u}{\partial \overline{z}} \overline{n}\right], \tag{16}
$$

in which t, u, and n are the complex traction, displacement and normal, respectively. In applying this formula, z and $\overline{z}$ are considered as two independent variables, that is, $\partial z/\partial \overline{z} = \partial \overline{z}/\partial z = 0$. It is straightforward to verify that Eq. (16) is indeed equivalent to Eq. (15) by simply extracting the real and imaginary parts of $t(z)$ from (16) and comparing with the results from expanding (15). A similar formula for the traction in the normal and tangential directions is given in [39] and further related discussions can be found in [38].

Applying the relation in Eq. (16), we can show that HBIE (5) can be written in the following complex form:

$$
\frac{1}{2}t(z_0) = F_t(z_0) - F_u(z_0), \tag{17}
$$

where

$$F_t(z_0) \equiv [F_1(\mathbf{x}) + iF_2(\mathbf{x})]_t \equiv \left[\int_S K_{1j}(\mathbf{x},\mathbf{y})t_j(\mathbf{y})dS(\mathbf{y})\right] + i\left[\int_S K_{2j}(\mathbf{x},\mathbf{y})t_j(\mathbf{y})dS(\mathbf{y})\right] = \frac{1}{2\pi(1+\kappa)} \int_S \left\{\left[G'(z_0,z)t(z) + \overline{G'(z_0,z)t(z)}\right] n(z_0) + \left[\kappa\overline{G'(z_0,z)}t(z) - (z_0-z)\,\overline{G''(z_0,z)t(z)}\right] \overline{n(z_0)}\right\} dS(z), \tag{18}$$

representing the first integral with the K kernel in HBIE (5), and

$$F_u(z_0) \equiv [F_1(\mathbf{x}) + iF_2(\mathbf{x})]_u \equiv \left[\int_S H_{1j}(\mathbf{x},\mathbf{y})u_j(\mathbf{y})dS(\mathbf{y})\right] + i\left[\int_S H_{2j}(\mathbf{x},\mathbf{y})u_j(\mathbf{y})dS(\mathbf{y})\right] = -\frac{\mu}{\pi(1+\kappa)} \int_S \left\{\left[G''(z_0,z)n(z)u(z) + \overline{G''(z_0,z)n(z)u(z)}\right] n(z_0) + \left[\overline{G''(z_0,z)}\left(n(z)\overline{u(z)} + \overline{n(z)}u(z)\right) - (z_0-z)\,\overline{G'''(z_0,z)n(z)u(z)}\right] \overline{n(z_0)}\right\} dS(z), \tag{19}$$

representing the second integral with the H kernel in HBIE (5).

In the following, we first review the multipole expansions, local expansions and their translations related to Eqs. (13) and (14) in the fast multipole BEM for CBIE (12). Then we derive the same results related to Eqs. (18) and (19) for HBIE (17).

(a) Multipole expansion for the U Kernel integral

Assuming z_c is a multipole expansion point close to z (Fig. 2), that is, $|z - z_c| << |z_0 - z_c|$, the *multipole expansion* for $D_t(z_0)$ in (13) with the U kernel is given by [16]:

$$D_t(z_0) = \frac{1}{4\pi\mu(1+\kappa)}\left[\kappa\sum_{k=0}^{\infty} O_k(z_0 - z_c)M_k(z_c) + z_0\sum_{k=0}^{\infty}\overline{O_{k+1}(z_0 - z_c)M_k(z_c)} + \sum_{k=0}^{\infty}\overline{O_k(z_0 - z_c)}N_k(z_c)\right], \tag{20}$$

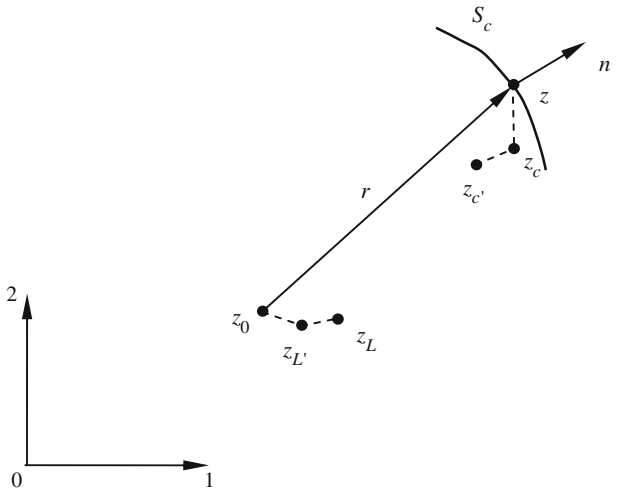

Fig. 2 Complex notation and the related points for fast multipole expansions

where

$$M_k(z_c) = \int_{S_c} I_k(z - z_c)t(z)dS(z), \quad \text{for } k \geq 0, \tag{21}$$

and

$$\begin{cases} N_0 = \kappa\int_{S_c} t(z)dS(z); \\ N_k(z_c) = \int_{S_c}\left[\kappa\overline{I_k(z - z_c)}t(z) - \overline{I_{k-1}(z - z_c)}\overline{zt(z)}\right] \\ \quad dS(z) \quad \text{for } k \geq 1. \end{cases} \tag{22}$$

are the two sets of moments about z_c with S_c being a subset of S that is far away from the source point [16]. The two auxiliary functions $I_k(z)$ and $O_k(z)$ are defined by:

$$I_k(z) = \frac{z^k}{k!}, \quad \text{for } k \geq 0; \tag{23}$$

$$O_0(z) = -\log(z); \text{ and } O_k(z) = \frac{(k-1)!}{z^k}, \quad \text{for } k \geq 1. \tag{24}$$

(b) Moment-to-moment (M2M) translation

If the multipole expansion point z_c is moved to a new location $z_{c'}$ (Fig. 2), we have [16]:

$$M_k(z_{c'}) = \sum_{l=0}^{k} I_{k-l}(z_c - z_{c'})M_l(z_c), \quad \text{for } k \geq 0. \tag{25}$$

Similarly,

$$N_k(z_{c'}) = \sum_{l=0}^{k}\overline{I_{k-l}(z_c - z_{c'})}N_l(z_c), \quad \text{for } k \geq 0. \tag{26}$$

These are the *M2M translations* for the moments when z_c is moved to $z_{c'}$. Note that these translation coefficients are symmetrical for the two sets of moments (I_{k-l} and conjugate of I_{k-l}) and coefficients I_{k-l} are exactly the same as used in the 2D potential case [3,15].

(c) Local expansion and moment-to-local (M2L) translation

If z_L is a local expansion point close to point z_0 (Fig. 2), that is, $|z_0 - z_L| \ll |z_c - z_L|$. Expanding $D_t(z_0)$ in (20) about $z_0 = z_L$ using Taylor series expansion, we have the following *local expansion* [16]:

$$D_t(z_0) = \frac{1}{4\pi\mu(1+\kappa)}\left[\kappa\sum_{l=0}^{\infty} L_l(z_L)I_l(z_0 - z_L) - z_0\sum_{l=1}^{\infty}\overline{L_l(z_L)I_{l-1}(z_0 - z_L)} + \sum_{l=0}^{\infty} K_l(z_L)\overline{I_l(z_0 - z_L)}\right], \tag{27}$$

where the coefficients are given by the following *M2L translations* [16]:

$$L_l(z_L) = (-1)^l\sum_{k=0}^{\infty} O_{l+k}(z_L - z_c)M_k(z_c), \quad \text{for } l \geq 0; \tag{28}$$

$$K_l(z_L) = (-1)^l\sum_{k=0}^{\infty}\overline{O_{l+k}(z_L - z_c)}N_k(z_c), \quad \text{for} l \geq 0. \tag{29}$$

(d) Local-to-local translation (L2L)

If the local expansion point is moved from z_L to $z_{L'}$ (Fig. 2), the new local expansion coefficients are given by the following *L2L translations* [16]:

$$L_l(z_{L'}) = \sum_{m=l}^{\infty} I_{m-l}(z_{L'} - z_L)L_m(z_L), \quad \text{for } l \geq 0; \tag{30}$$

$$K_l(z_{L'}) = \sum_{m=l}^{\infty}\overline{I_{m-l}(z_{L'} - z_L)}K_m(z_L), \quad \text{for } l \geq 0. \tag{31}$$

(e) Expansions for the T Kernel integral

Through a similar procedure as used for the U kernel integral in (13), the multipole expansion of T kernel integral $D_u(z_0)$ in (14) can be written as [16]:

$$D_u(z_0) = \frac{1}{2\pi(1+\kappa)}\left[\kappa\sum_{k=1}^{\infty} O_k(z_0 - z_c)\tilde{M}_k(z_c) + z_0\sum_{k=1}^{\infty}\overline{O_{k+1}(z_0 - z_c)}\overline{\tilde{M}_k(z_c)} + \sum_{k=1}^{\infty}\overline{O_k(z_0 - z_c)}\tilde{N}_k(z_c)\right], \tag{32}$$

where the two sets of *moments* are:

$$\tilde{M}_k(z_c) = \int_{S_c} I_{k-1}(z - z_c)n(z)u(z)dS(z), \quad \text{for } k \geq 1; \tag{33}$$

$$\begin{cases}\tilde{N}_1 = \int_{S_c}\left[n(z)\overline{u(z)} + \overline{n(z)}u(z)\right]dS(z); \\ \tilde{N}_k(z_c) = \int_{S_c}\left\{\overline{I_{k-1}(z - z_c)}\left[n(z)\overline{u(z)} + \overline{n(z)}u(z)\right] - \overline{I_{k-2}(z - z_c)}z\overline{n(z)u(z)}\right\}dS(z), \quad \text{for } k \geq 2.\end{cases} \tag{34}$$

These moments are similar to those for the U kernel integral. It can be shown that the M2M, M2L and L2L translations remain the same for the T kernel integrals, except for the fact that $\tilde{M}_0 = \tilde{N}_0 = 0$. The local expansion for $D_u(z_0)$ is:

$$D_u(z_0) = \frac{1}{2\pi(1+\kappa)}\left[\kappa\sum_{l=0}^{\infty} L_l(z_L)I_l(z_0 - z_L) - z_0\sum_{l=1}^{\infty}\overline{L_l(z_L)I_{l-1}(z_0 - z_L)} + \sum_{l=0}^{\infty} K_l(z_L)\overline{I_l(z_0 - z_L)}\right], \tag{35}$$

where the local expansion coefficients $L_l(z_L)$ and $K_l(z_L)$ are given by Eqs. (28) and (29) with M_k being replaced by $\tilde{M}_k$, and N_k by $\tilde{N}_k$, respectively.

(f) Expansions for the HBIE

To derive the multipole expansions and local expansions for HBIE (17), one can simply take the derivatives of the local expansions for the two integrals in the CBIE, that is, Eqs. (27) and (35), respectively, and then invoke the constitutive relation in the complex form (Eq. 16). The result of the local expansion for the first integral $F_t(z_0)$ in (18) for the HBIE is:

$$F_t(z_0) = \frac{1}{2\pi(1+\kappa)}\left\{\left[\sum_{l=0}^{\infty} L_{l+1}(z_L)I_l(z_0 - z_L) + \sum_{l=0}^{\infty}\overline{L_{l+1}(z_L)I_l(z_0 - z_L)}\right]n(z_0) + \left[-z_0\sum_{l=1}^{\infty}\overline{L_{l+1}(z_L)I_{l-1}(z_0 - z_L)} + \sum_{l=0}^{\infty} K_{l+1}(z_L)\overline{I_l(z_0 - z_L)}\right]\overline{n(z_0)}\right\}, \tag{36}$$

in which, the expansion coefficients $L_l(z_L)$ and $K_l(z_L)$ are given by the same M2L translations in (28) and (29), respectively. That is, the same sets of moments M_k and N_k used for $D_t(z_0)$ are used for $F_t(z_0)$ directly. Similarly, it can be shown that the local expansion for the second integral $F_u(z_0)$ in (19) for the HBIE is:

$$F_u(z_0) = \frac{\mu}{\pi(1+\kappa)} \left\{ \left[\sum_{l=0}^{\infty} L_{l+1}(z_L) I_l(z_0 - z_L) + \sum_{l=0}^{\infty} \overline{L_{l+1}(z_L) I_l(z_0 - z_L)} \right] n(z_0) + \left[-z_0 \sum_{l=1}^{\infty} \overline{L_{l+1}(z_L) I_{l-1}(z_0 - z_L)} + \sum_{l=0}^{\infty} K_{l+1}(z_L) \overline{I_l(z_0 - z_L)} \right] \overline{n(z_0)} \right\}, \quad (37)$$

where $L_l(z_L)$ and $K_l(z_L)$ are given by Eqs. (28) and (29) with M_k being replaced by $\tilde{M}_k$, and N_k by $\tilde{N}_k$, respectively. Again, the same moments $\tilde{M}_k$ and $\tilde{N}_k$ used for $D_u(z_0)$ are used for $F_u(z_0)$, and all the M2M, M2L and L2L translations for the CBIE are used for the HBIE.

The details of the fast multipole algorithms for solving 2D elasticity problems have been described in details in [16]. In this study, constant boundary elements (straight line segment with one node) are applied to discretize the BIEs. All the moments are evaluated analytically, as well as the integrations of the kernels in the near-field direct evaluations.

Pre-conditioners for the fast multipole BEM are crucial for its convergence and computing efficiency. In this study, two pre-conditioners are devised based on the two forms of the BEM system of equations shown in Eqs. (10) and (11).

For *Pre-conditioner A*, a block diagonal pre-conditioner based on Eq. (10) is employed. For the matrix domain, a diagonal submatrix is formed on each leaf using direct evaluations of the kernels on the elements within that leaf, while for the inclusions, the submatrix $\mathbf{B}_i^f$ in Eq. (10) along the main diagonal is used for each inclusion.

For *Pre-conditioner B*, a block diagonal pre-conditioner based on Eq. (11) is employed. In this case, the following matrix from the matrix in Eq. (11) is used as the pre-conditioner:

$$\mathbf{M} = \begin{bmatrix} \mathbf{A}_{00} & \mathbf{0} & \mathbf{0} & \mathbf{0} & \mathbf{0} & \cdots & \mathbf{0} & \mathbf{0} \\ \mathbf{0} & \mathbf{A}_{11} & -\mathbf{B}_{11} & \mathbf{0} & \mathbf{0} & \cdots & \mathbf{0} & \mathbf{0} \\ \mathbf{0} & \mathbf{A}_1^f & \mathbf{B}_1^f & \mathbf{0} & \mathbf{0} & \cdots & \mathbf{0} & \mathbf{0} \\ \mathbf{0} & \mathbf{0} & \mathbf{0} & \mathbf{A}_{22} & -\mathbf{B}_{22} & \cdots & \mathbf{0} & \mathbf{0} \\ \mathbf{0} & \mathbf{0} & \mathbf{0} & \mathbf{A}_2^f & \mathbf{B}_2^f & \cdots & \mathbf{0} & \mathbf{0} \\ \vdots & \vdots & \vdots & \vdots & \vdots & \ddots & \vdots & \vdots \\ \mathbf{0} & \mathbf{0} & \mathbf{0} & \mathbf{0} & \mathbf{0} & \cdots & \mathbf{A}_{nn} & -\mathbf{B}_{nn} \\ \mathbf{0} & \mathbf{0} & \mathbf{0} & \mathbf{0} & \mathbf{0} & \cdots & \mathbf{A}_n^f & \mathbf{B}_n^f \end{bmatrix}. \quad (38)$$

This pre-conditioner is equivalent to solving many inclusion problems as if there is only one inclusion embedded in an infinite domain in each case. For this pre-conditioner, larger diagonal matrices need to be inverted for each inclusion, which can be time-consuming if the number of elements on each inclusion is large. However, this pre-conditioner is very effective for inclusion problems because the number of iterations for the GMRES solver can be reduced significantly, as will be shown in the third numerical example in the next section. A similar pre-conditioner has been applied in the 3D fast multipole BEM for modeling rigid-inclusion problems using the 3D single-domain CBIE [40,41].

The systems in Eqs. (10) and (11) are right pre-conditioned with the above two pre-conditioners, respectively. LU decompositions of the submatrices in these pre-conditioners are obtained once and saved in memory in the subsequent iterations to save the CPU time.

4 Numerical examples

We present several numerical examples to demonstrate the accuracy and efficiency of the new fast multipole BEM for 2D multi-domain elasticity problems using the dual BIE formulation. In all the examples, the number of terms for both multipole and local expansions is set to 20, maximum number of elements in a leaf to 100, tolerance for convergence to 10^{-6}, and coupling constant β for the dual BIE (CHBIE) formulation to a typical element size in the mesh.

(a) A concentric cylinder model

We first study a concentric cylinder model (Fig. 3) to verify the CHBIE formulation for multi-domain problems. In this case, a solid cylinder (e.g., a fiber) is embedded in a larger cylinder (e.g., a matrix) with the parameters: $a = 1, b = 2$, Young's modulus $E = 1$ and Poisson's ratio $\nu = 0.3$ for the matrix, and $E = 2$ and $\nu = 0.3$ for the inclusion. The model is applied with a radial displacement $u_r = 1$ on the outer boundary S_b. Plane strain condition is assumed. For this problem, the analytical solution is available (see, e.g., [42]).

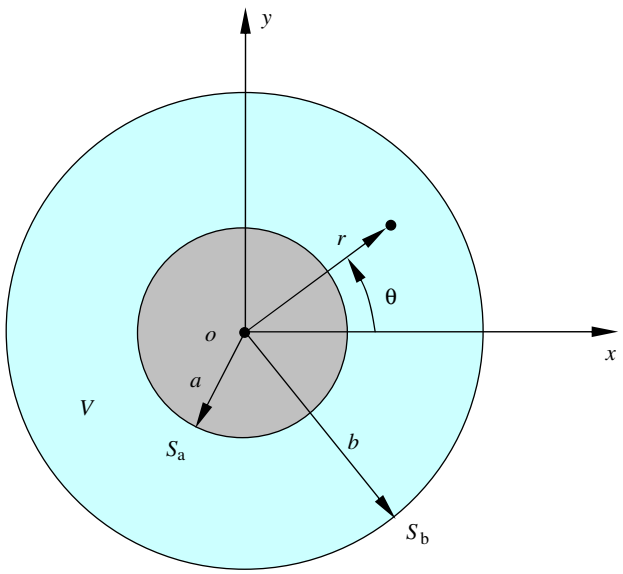

Fig. 3 A concentric cylinder model

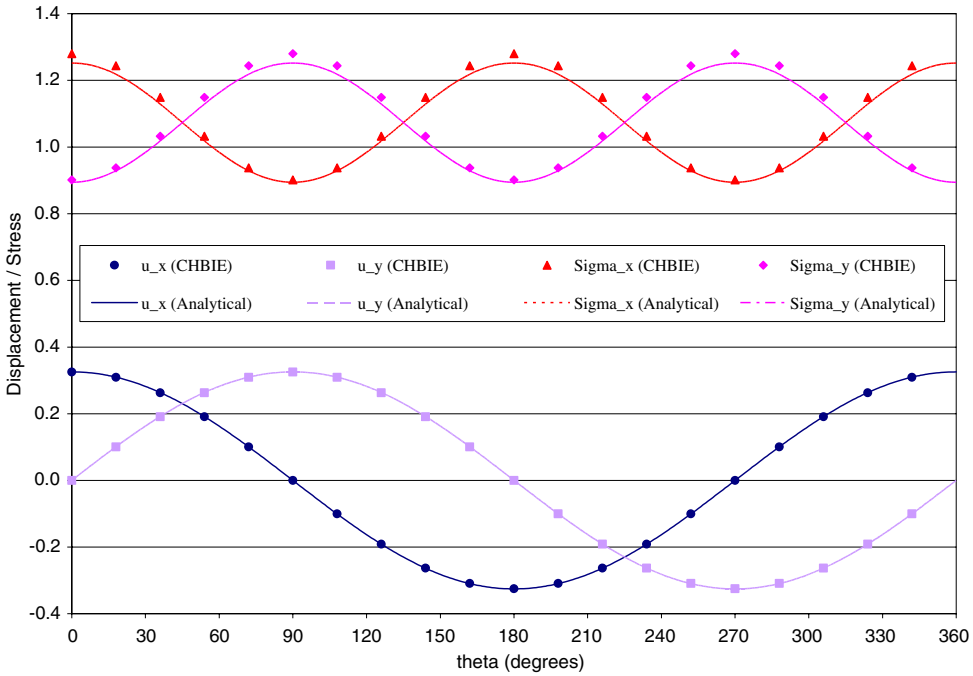

Fig. 4 Distributions of displacements and stresses in the matrix along the interface ($r = a$) with 60 boundary elements

Table 1 Displacement and stresses in the outer cylinder at the interface ($r = a$)

Total no. of elements	Total DOFs	u_r		σ_r		σ_θ	
		CBIE	CHBIE	CBIE	CHBIE	CBIE	CHBIE
60	120	0.32622	0.32510	1.29146	1.28023	0.90755	0.90152
120	240	0.32629	0.32580	1.26852	1.26519	0.90111	0.89914
180	360	0.32614	0.32589	1.26234	1.26084	0.89891	0.89799
240	480	0.32603	0.32588	1.25953	1.25863	0.89780	0.89724
300	600	0.32596	0.32585	1.25794	1.25734	0.89713	0.89676
600	1, 200	0.32578	0.32576	1.25495	1.25479	0.89580	0.89570
1,200	2, 400	0.32569	0.32568	1.25356	1.25352	0.89513	0.89510
2,400	4, 800	0.32564	0.32563	1.25289	1.25288	0.89479	0.89478
3,000	6, 000	0.32562	0.32562	1.25276	1.25275	0.89472	0.89472
6,000	12, 000	0.32560	0.32560	1.25250	1.25250	0.89459	0.89459
9,000	18, 000	0.32560	0.32560	1.25241	1.25240	0.89456	0.89451
Exact solution		0.32558		1.25224		0.89445	

Table 1 shows the results of the displacement and stresses in the matrix domain and at the interface S_a by the fast multipole BEM using both the CBIE and CHBIE formulations with the total number of elements used on both the boundary and interface changing from 60 to 3,000. Both BIE formulations give results of comparable accuracies. With only 60 elements on the outer boundary and the interface (20 elements on each boundary curve of each domain) , the errors in the BEM results (σ_r) are less than 3%. Figure 4 is a plot of the displacement and stress components on the interface from the matrix domain with the 60-element mesh and using the CHBIE. The stress data for σ_x and σ_y in Fig. 4 and for σ_θ in Table 1 are computed based on the boundary values of the displacement and traction fields using interpolations. These results demonstrate that the multi-domain fast multipole BEM is fairly accurate and stable within a large range of mesh densities.

(b) A plate with an elliptical inclusion

We next study a square plate embedded with an elliptical inclusion at the center (Fig. 5) to further test the accuracy and robustness of the dual BIE formulation. If the Young's modulus of the inclusion is much smaller than that of the plate, the problem is close to the case of a plate with a very

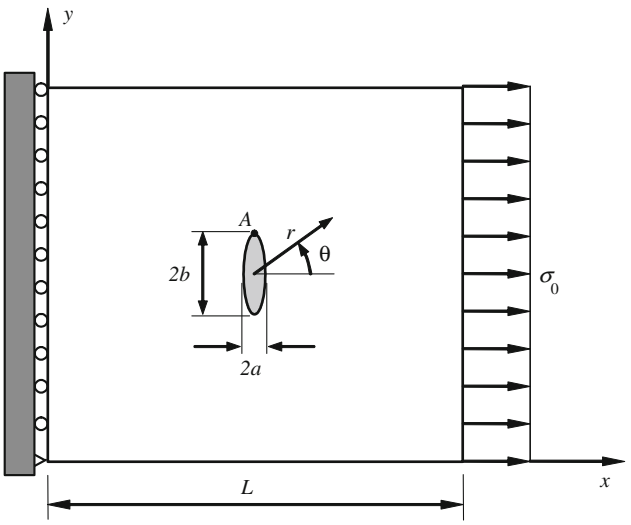

Fig. 5 A square plate with a very "soft" elliptical inclusion at the center and loaded with σ_0

"soft" inclusion or with an elliptical hole, for which analytical solutions can be used to verify the results. The dimensions used are: $L = 1, b = 0.025, E = 1$ and $\nu = 0.3$ for the plate, and $E = 0.00001$ and $\nu = 0.3$ for the inclusion. Plane stress condition is assumed.

We first calculate the maximum hoop stress along the edge the "hole" with various values of a/b. This maximum stress is at point A (Fig. 5) and the analytical value for an infinitely large plate with an elliptical hole is $\sigma_{\max} = \sigma_0(1+2b/a)$. The computed results using the BEM are listed in Table 2 for five values of a/b. A total of 100 elements are used on the outer boundary of the plate, while the number of elements on the interface (or edge of the "hole") changing from 100 to 1,600 with a decreasing ratio a/b. Good results are obtained using both the CBIE and CHBIE formulations. When the ratio a/b is below 0.05, stress field changes vary rapidly and large number of elements are required to capture these variations. Figure 6 shows the hoop stress (computed using boundary displacement and traction fields) on the edge of the "hole" when $a/b = 1$ and compared with the analytical solution for an infinitely large plate with a circular hole. There are 100 elements on the edge of the "hole" in this case. When a/b is small, the "hole" becomes an open crack with length $2b$ and the maximum stress tends to infinity at point A. Figure 7 shows the crack opening displacement (COD) for $a/b = 0.01$ with the CHBIE and compared with the analytical solution for the true crack case ($a/b = 0$). The results in Figs. 6 and 7 with the CHBIE agree very well with the corresponding analytical solutions.

This example further demonstrates that the dual BIE formulation can provide accurate solutions even when the domain of consideration is very thin and there is a large difference between the material properties for the different domains. This is consistent with the conclusions with the dual BIE formulations for solving thin-shape and crack problems [31,43].

(c) Multiple inclusion problems

We next study multiple inclusion problems using the dual BIE and the fast multipole BEM. The same domain and boundary conditions as in the previous example are studied. Two cases are considered here, one with multiple circular inclusions (long and unidirectional fibers) under plane strain condition, and the other with multiple crack-like inclusions under plane stress condition. Similar studies on multiple elastic inclusions of 2D elasticity using Kolosov–Muskhelishvili potentials can be found [44–46].

For the circular inclusion case the parameters used are: $a = b = 0.2$, fiber volume fraction = 12.57%, $E = 1$ and $\nu = 0.25$ for the matrix, and $E = 10$ and $\nu = 0.25$ for the inclusions. For the crack-like inclusion case, $b = 0.2$, $a/b = 0.01$, crack density = $b^2 = 4\%$, $E = 1$ and $\nu = 0.25$ for the matrix, and $E = 0.00001$ and $\nu = 0.25$ for the inclusions (cracks). In both cases, the inclusions are randomly distributed in the material domains (The cracks, however, are aligned). Two BEM models for the two cases are shown in Fig. 8. For the outer boundary 400 elements are used, and on each interface 200 elements are used. Using more elements on the outer boundary did not yield significant improvements in the evaluated effective properties of the materials discussed below.

The effective Young's moduli of the materials containing the circular inclusions and cracks in the x–y plane are evaluated using the fast multipole BEM with the CHBIE and compared with the estimates using homogenization theories which are based on dilute defect distributions ([47], Table 8.1). To compute the effective moduli E_x, the domain is fixed at the left edge and applied with a uniform load on the right edge. Averaged strain are computed from the boundary solution and then used to estimate the effective modulus (see [16]). Table 3 shows the BEM results with different numbers of the inclusions in the models and excellent results are obtained for both cases. With the increase of the size of the models, the evaluated effective Young's moduli approach constant values which are close to the analytical estimates in [47], as expected.

Figure 9 is a plot of the CPU times used for the calculations using the fast multipole BEM for the two cases studied and with the two pre-conditioners. The computer used for these calculations is with an Intel Pentium D 3.2 GHz processor and 2 GB memory size. For the circular inclusion case, the numbers of iterations using pre-conditioner A range from 141 to 550, while those using pre-conditioner B range from 11 to 16, with the tolerance of 10^{-6}. For the crack-like inclusion case, the numbers of iterations using pre-conditioner A range from 29 to 41, while those using pre-conditioner B range from

Table 2 Computed hoop stress σ_x (x σ_0) in the plate at point A

a/b	No. elements on interface	Total DOFs	σ_x (x σ_0) at point A		
			CBIE	CHBIE	Analytical
1.0	100	600	3.01	3.01	3.00
0.5	200	1,000	5.01	5.03	5.00
0.1	500	2,200	21.06	21.42	21.00
0.05	800	3,400	41.17	41.58	41.00
0.01	1,600	6,600	206.78	207.65	201.00

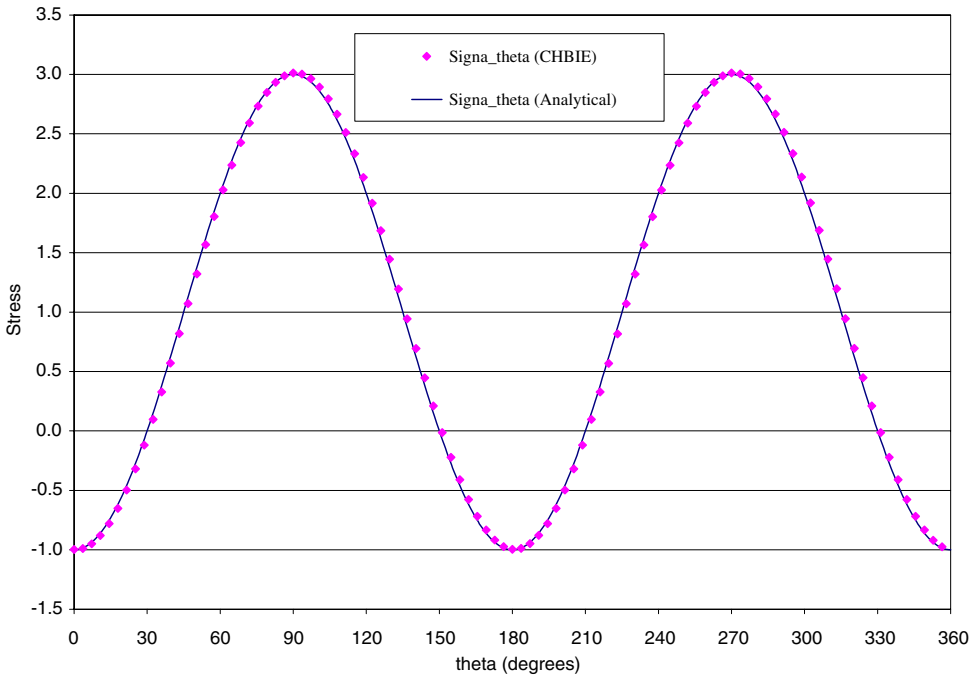

Fig. 6 Hoop stress around the edge of the "hole" when $a/b = 1$

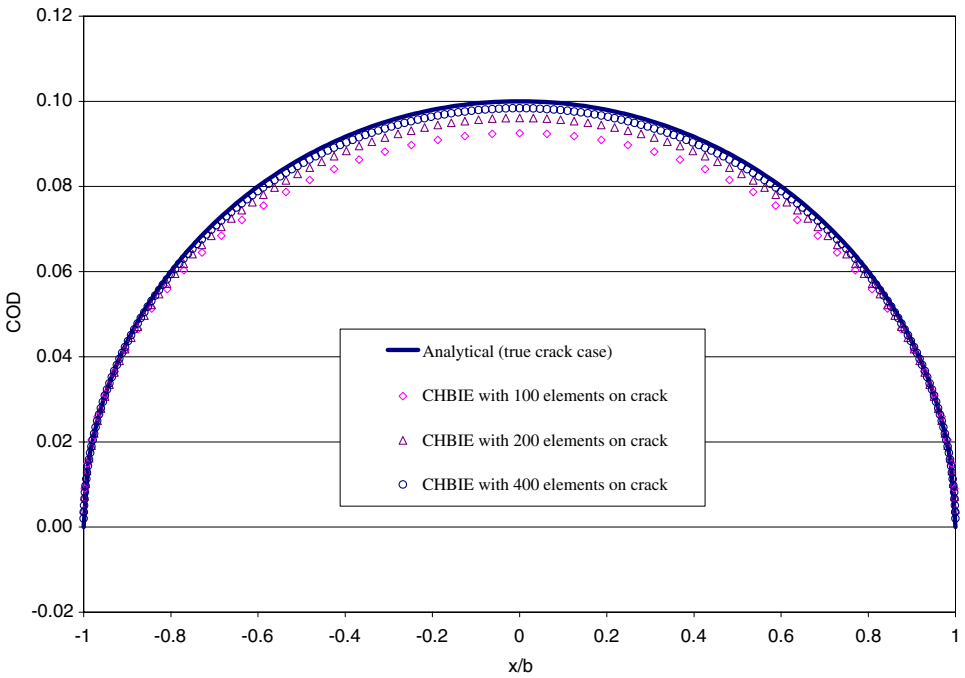

Fig. 7 Crack opening displacement (COD) when $a/b = 0.01$

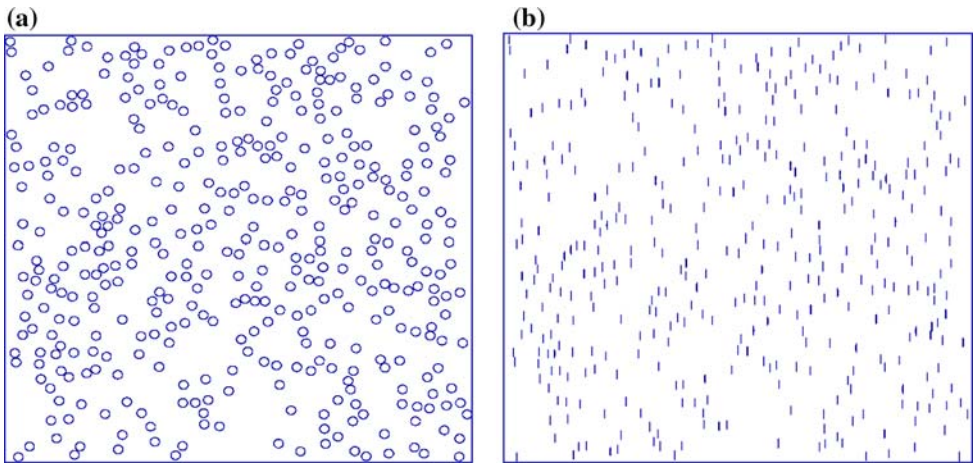

Fig. 8 Elastic domains embedded with elastic inclusions: (**a**) circular inclusions (*fibers*) with $E_i/E_0 = 10$; (**b**) crack-like inclusions with $E_i/E_0 = 0.00001$ and $a/b = 0.01$

Table 3 Computed effective moduli for the materials with circular and crack-like inclusions

No. of inclusions	Total DOFs	Effective moduli $E_x(\times E_0)$	
		Circular inclusions	Crack-like inclusions
2×2	4,000	1.2678	0.7631
4×4	13,600	1.2728	0.8024
6×6	29,600	1.2596	0.7808
8×8	52,000	1.2605	0.7923
10×10	80,800	1.2649	0.7891
12×12	116,000	1.2640	0.7902
14×14	157,600	1.2635	0.7886
16×16	205,600	1.2651	0.7900
18×18	260,000	1.2642	0.7897
20×20	320,800	1.2644	0.7885
Analytical estimates [47]		1.2491	0.7992

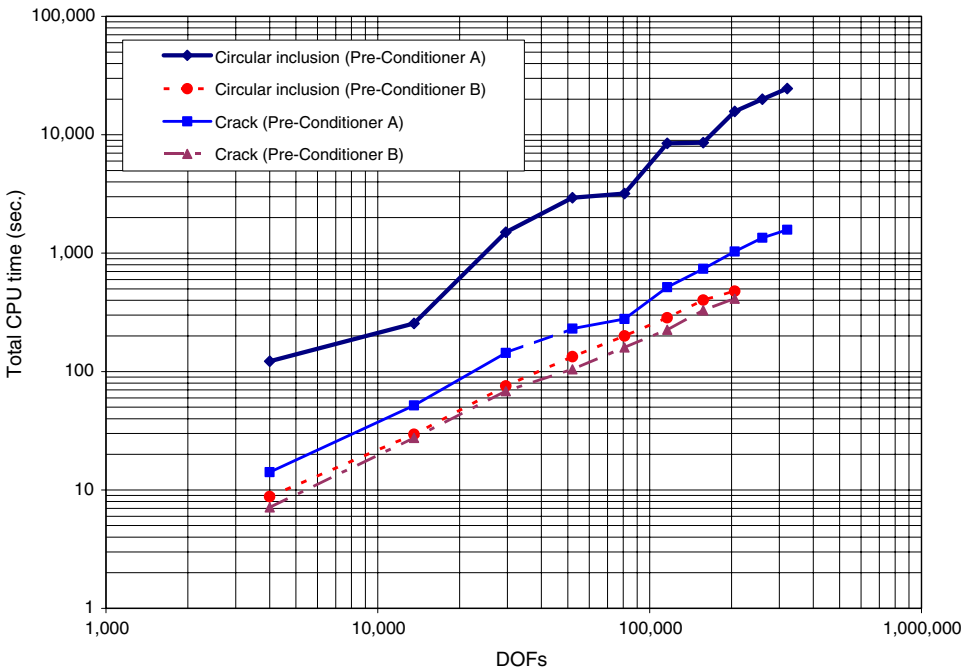

Fig. 9 CPU times used for the multiple circular and crack-like inclusion models

12 to 14. Significant advantages of using pre-conditioner B are observed in both cases. However, larger memory size are needed for using pre-conditioner B when the LU decompositions are saved in core as in this study. The last two larger models are not solved by the BEM with pre-conditioner B due to this constraint with the computer used. It is also observed that the dual BIE provides much better conditioning for the crack-like inclusion problems, based on the fact that much faster convergence is achieved for the crack-like inclusion problem than for the circular inclusion problem.

These results clearly demonstrate the accuracy and efficiency of the fast multipole BEM with the dual BIE formulation for solving large-scale multi-domain 2D elasticity problems.

5 Discussions

A new fast multipole BEM approach for solving large-scale multi-domain 2D elasticity problems using a dual BIE formulation is presented in this paper, based on the work in [16] which is for 2D single-domain problems with the CBIE only. The fast multipole formulations are presented in this paper for both the CBIE and HBIE for the 2D elasticity problems. These formulations are based on a complex variable approach that yields very compact results. For the HBIE, local expansions can be obtained by directly taking derivatives of the local expansions for the CBIE using the complex notation. The same moments and all M2M, M2L and L2L translations as used for the CBIE can be applied for the HBIE. Three numerical examples are presented that clearly demonstrate the accuracy and efficiency of the developed fast multipole BEM with the dual BIE for solving large-scale multi-domain 2D elasticity problems.

Multi-domain problems present new challenges to the fast multipole BEM due to the less favorable conditioning of the systems of BEM equations. Due to the mismatch of the material properties in different domains, the conditioning of the BEM systems can deteriorate. Careful selection of the systems of equations to be used with the fast multipole BEM is critical for solving multi-domain problems. The pre-conditioner B in Eq. (37), which is based on the BEM system in Eq. (11), is found to be very efficient in reducing the number of iterations in the fast multipole BEM solutions, although it requires larger memory size if the pre-conditioners are to be stored in memory in order to reduce the CPU time. For special cases, for example, when all the inclusions have the same geometry and same material properties, the BIE equations for the inclusions can be solved once and eliminated from the whole system of the equations for the multi-domain problems, leaving only the equations from the matrix domain to be solved using the fast multipole BEM (see, e.g., [19]). However, this simplification is not applied in this current work with the intent to leave the developed fast multipole BEM code as general as possible so that it can be applied to solve a broader range of 2D elasticity problems, such as modeling of functional-grade materials with inclusions having different geometries and mechanical properties.

To improve the accuracy and efficiency of the fast multipole BEM for solving large-scale models, higher-order elements (such as linear and quadratic elements) can be applied to replace the constant elements. For problems with curved boundaries or slender structures in bending, use of constant elements for the displacement fields is not efficient and large number of elements may be needed. Using higher-order elements will be especially beneficial to the HBIE since the finite-part integrals can be evaluated more accurately on curved boundaries with higher-order elements than with the constant elements as used in this study. Parallel computing with the fast multipole BEM [5,8,48] can also be employed to further improve the computational efficiencies. Field evaluations inside the domain can be performed with the fast multipole BEM as well [49].

The developed dual BIE approach together with the efficient fast multipole BEM can be extended to study other 2D problems, such as modeling of composite materials, functionally-graded materials (FGMs), and micro-electro-mechanical-systems (MEMS), all of which often involve thin inclusions. The developed code can also be applied to study crack propagation problems [17] which can have significant advantages over other methods. Combining the fast multipole BEM code for elasticity problems with the potential [15,50] or Stokes flow [35] code to study coupled fluid–structure interaction problems is also possible and will be an interesting research topic for applications in analyzing MEMS devices and biological systems.

Acknowledgments This research has been supported by grant CMS-0508232 of the US National Science Foundation which is gratefully acknowledged. The author would also like to thank the two reviewers for their constructive comments on this work.

References

1. Rokhlin V (1985) Rapid solution of integral equations of classical potential theory. J Comp Phys 60:187–207
2. Greengard LF, Rokhlin V (1987) A fast algorithm for particle simulations. J Comput Phys 73(2):325–348
3. Greengard LF (1988) The rapid evaluation of potential fields in particle systems. MIT Press, Cambridge
4. Peirce AP, Napier JAL (1995) A spectral multipole method for efficient solution of large-scale boundary element models in elastostatics. Int J Numer Meth Eng 38:4009–4034
5. Gomez JE, Power H (1997) A multipole direct and indirect BEM for 2D cavity flow at low Reynolds number. Eng Anal Bound Elem 19:17–31
6. Fu Y, Klimkowski KJ, Rodin GJ, Berger E, Browne JC, Singer JK, Geijn RAVD, Vemaganti KS (1998) A fast solution method for three-dimensional many-particle problems of linear elasticity. Int J Numer Meth Eng 42:1215–1229

7. Nishimura N, Yoshida K, Kobayashi S (1999) A fast multipole boundary integral equation method for crack problems in 3D. Eng Anal Bound Elem 23:97–105
8. Mammoli AA, Ingber MS (1999) Stokes flow around cylinders in a bounded two-dimensional domain using multipole-accelerated boundary element methods. Int J Numer Meth Eng 44:897–917
9. Nishimura N (2002) Fast multipole accelerated boundary integral equation methods. Appl Mech Rev 55(4):299–324
10. Greengard LF, Kropinski MC, Mayo A (1996) Integral equation methods for Stokes flow and isotropic elasticity in the plane. J Comput Phys 125:403–414
11. Greengard LF, Helsing J (1998) On the numerical evaluation of elastostatic fields in locally isotropic two-dimensional composites. J Mech Phys Solids 46(8):1441–1462
12. Richardson JD, Gray LJ, Kaplan T, Napier JA (2001) Regularized spectral multipole BEM for plane elasticity. Eng Anal Bound Elem 25:297–311
13. Fukui T (1998) Research on the boundary element method—development and applications of fast and accurate computations. Ph.D. dissertation (in Japanese), Department of Global Environment Engineering, Kyoto University
14. Fukui T, Mochida T, Method K (1997) Crack extension analysis in system of growing cracks by fast multipole boundary element method (in Japanese), Seventh BEM technology conference (JASCOME, Tokyo, 1997) pp 25–30
15. Liu YJ, Nishimura N (2006) The fast multipole boundary element method for potential problems: a tutorial. Eng Anal Bound Elem 30(5):371–381
16. Liu YJ (2005) A new fast multipole boundary element method for solving large-scale two-dimensional elastostatic problems. Int J Numer Meth Eng 65(6):863–881
17. Wang P, Yao Z (2006) Fast multipole DBEM analysis of fatigue crack growth. Computat Mech 38:223–233
18. Yamada Y, Hayami K (1995) A multipole boundary element method for two dimensional elastostatics. Report METR 95–07, Department of Mathematical Engineering and Information Physics, University of Tokyo
19. Yao Z, Kong F, Wang H, Wang P (2004) 2D simulation of composite materials using BEM. Eng Anal Bound Elem 28(8):927–935
20. Wang J, Crouch SL, Mogilevskaya SG (2005) A fast and accurate algorithm for a Galerkin boundary integral method. Comput Mech 37(1):96
21. Rizzo FJ (1967) An integral equation approach to boundary value problems of classical elastostatics. Q Appl Math 25:83–95
22. Mukherjeec S (1982) Boundary element methods in creep and fracture. Applied Science Publishers, New York
23. Cruse TA (1988) Boundary element analysis in computational fracture mechanics. Kluwer, Dordrecht
24. Brebbia CA, Dominguez J (1989) Boundary elements—an introductory course. McGraw-Hill, New York
25. Banerjee PK (1994) The boundary element methods in engineering, 2nd edn. McGraw-Hill, New York
26. Krishnasamy G, Rizzo FJ, Rudolphi TJ (1991) Hypersingular boundary integral equations: their occurrence, interpretation, regularization and computation. In: Banerjee PK et al (eds) Developments in boundary element methods, Chap 7. Elsevier, London
27. Sladek V, Sladek J (eds) (1998) Singular integrals in boundary element methods. In: Brebbia CA, Aliabadi MH (eds) Advances in boundary element series, Computational Mechanics Publications, Boston
28. Mukherjee S (2000) Finite parts of singular and hypersingular integrals with irregular boundary source points. Eng Anal Bound Elem 24:767–776
29. Liu YJ, Rizzo FJ (1992) A weakly-singular form of the hypersingular boundary integral equation applied to 3-D acoustic wave problems. Comp Meth Appl Mech Eng 96:271–287
30. Liu YJ, Rizzo FJ (1993) Hypersingular boundary integral equations for radiation and scattering of elastic waves in three dimensions. Comp Meth Appl Mech Eng 107:131–144
31. Liu YJ, Rizzo FJ (1997) Scattering of elastic waves from thin shapes in three dimensions using the composite boundary integral equation formulation. J Acoust Soc Am 102(2), No. Pt.1, August, 926–932
32. Shen L, Liu YJ (2007) An adaptive fast multipole boundary element method for three-dimensional acoustic wave problems based on the Burton–Miller formulation. Comput Mech 40(3): 461–472
33. Liu YJ (2006) Dual BIE approaches for modeling electrostatic MEMS problems with thin beams and accelerated by the fast multipole method. Eng Anal Bound Elem 30(11):940–948
34. Liu YJ, Shen L (2007) A dual BIE approach for large-scale modeling of 3-D electrostatic problems with the fast multipole boundary element method. Int J Numer Meth Eng 71(7):837–855
35. Liu YJ (2008) A new fast multipole boundary element method for solving 2D Stokes flow problems based on a dual BIE formulation. Eng Anal Bound Elem 32(2):139–151
36. Muskhelishvili NI (1958) Some basic problems of mathematical theory of elasticity. Noordhoff, Groningen
37. Sokolnikoff IS (1956) Mathematical theory of elasticity. McGraw Hill, New York
38. Mogilevskaya SG, Linkov AM (1998) Complex fundamental solutions and complex variables boundary element method in elasticity. Comput Mech 22(1):88–92
39. Linkov AM, Mogilevskaya SG (1998) Complex hypersingular BEM in plane elasticity problems. In: Sladek V, Sladek J (eds) Singular integrals in boundary element method. Computational Mechanics Publications, Southampton pp 299–364
40. Liu YJ, Nishimura N, Otani Y, Takahashi T, Chen XL, Munakata H (2005) A fast boundary element method for the analysis of fiber-reinforced composites based on a rigid-inclusion model. J Appl Mech 72(1):115–128
41. Liu YJ, Nishimura N, Otani Y (2005) Large-scale modeling of carbon-nanotube composites by the boundary element method based on a rigid-inclusion model. Comput Mater Sci 34(2):173–187
42. Liu YJ, Xu N, Luo JF (2000) Modeling of interphases in fiber-reinforced composites under transverse loading using the boundary element method. J Appl Mech 67(1):41–49
43. Krishnasamy G, Rizzo FJ, Liu YJ (1994) Boundary integral equations for thin bodies. Int J Numer Meth Eng 37:107–121
44. Wang J, Mogilevskaya SG, Crouch SL (2003) Benchmarks results for the problem of interaction between a crack and a circular inclusion. J Appl Mech 70:619–621
45. Mogilevskaya SG, Crouch SL (2004) A Galerkin boundary integral method for multiple circular elastic inclusions with uniform interphase layers. Int J Solids Struct 41:1285–1311
46. Wang J, Mogilevskaya SG, Crouch SL (2005) An embedding method for modeling micromechanical behavior and macroscopic properties of composite materials. Int J Solids Struct 42:4588–4612
47. Gross D, Seelig T (2006) Fracture mechanics with an introduction to micromechanics. Springer, The Netherlands
48. Gomez JE, Power H (2000) A parallel multipolar indirect boundary element method for the Neumann interior Stokes flow problem. Int J Numer Meth Eng 48(4):523–543
49. Yoshida K, Nishimura N, Kobayashi S (2001) Application of fast multipole Galerkin boundary integral equation method to crack problems in 3D. Int J Numer Meth Eng 50:525–547
50. Shen L, Liu YJ (2007) An adaptive fast multipole boundary element method for three-dimensional potential problems. Comput Mech 39(6):681–691